Separation Science and Technology
Publication details, including instructions for authors and subscription information:
http://www.informaworld.com/smpp/title~content=t713708471

Dynamic Membranes. I. Determination of Optimum Formation Conditions and Electrofiltration of Bovine Serum Albumin with a Rotating Module

A. K. Turkson[ab]; J. A. Mikhlin[a]; M. E. Weber[a]
[a] DEPARTMENT OF CHEMICAL ENGINEERING, McGILL UNIVERSITY, MONTREAL, QUEBEC, CANADA [b] Département de Génie Chimique, Ecole Polytechnique de Montréal, Montréal, Québec, Canada

To cite this Article Turkson, A. K. , Mikhlin, J. A. and Weber, M. E.(1989) 'Dynamic Membranes. I. Determination of Optimum Formation Conditions and Electrofiltration of Bovine Serum Albumin with a Rotating Module', Separation Science and Technology, 24: 15, 1261 — 1291
To link to this Article: DOI: 10.1080/01496398908050651
URL: http://dx.doi.org/10.1080/01496398908050651

SEPARATION SCIENCE AND TECHNOLOGY, 24(15), pp. 1261-1291, 1989/90

Dynamic Membranes. I. Determination of Optimum Formation Conditions and Electrofiltration of Bovine Serum Albumin with a Rotating Module

A. K. TURKSON,* J. A. MIKHLIN,† and M. E. WEBER‡

DEPARTMENT OF CHEMICAL ENGINEERING
McGILL UNIVERSITY
MONTREAL, QUEBEC, CANADA

Abstract

The formation conditions were determined at which four dynamic membranes, Zr(IV) oxide, calcium oleate, poly-2-vinylpyridine, and cadmium sulfide, gave the largest fluxes coupled with rejections above 80% during filtration of bovine serum albumin. These membranes were selected because they were found to be stable in the presence of a dc electric field which was imposed between a rotating filter element and a stationary housing. The effects of electric field strength, rotation rate of the cylindrical filter element, and feed concentration were determined for the four membranes formed at their optimum conditions.

INTRODUCTION

Ultrafiltration is a pressure-driven filtration process in which the size of the dispersed phase is between 10 Å and 10 μm. Crossflow filtration and axial filtration are two fluid management techniques developed to minimize accumulation of the dispersed phase on the membrane. In crossflow filtration the feed flows at high velocity past the membrane surface, producing 1) turbulent eddies which increase solute diffusion away from

*Present address: Département de Génie Chimique, Ecole Polytechnique de Montréal, Montréal, Québec, Canada.

†Deceased.

‡To whom correspondence should be addressed.

the membrane and 2) shear stresses which may tear chunks of the solute layer from the filter. This technique was developed by Zhevnovatyi (*1*). In axial filtration a porous cylinder serving as the filter element rotates within a stationary housing. The feed enters the annular space while the filtrate is removed from inside the rotating porous cylinder. In addition to the generation of turbulent eddies and surface shear stresses, rotation of the cylinder produces centrifugal forces which move solute particles or molecules away from the membrane if the density of the solute is greater than the density of the fluid. Bhagat and Wilke (*2*) were the first to describe a porous, rotating, cylindrical filter element which they used in a fermentor called a rotorfermentor. The device has since seen several applications including desalination (*3*), ultrafiltration (*4*), and separation of oily emulsions (*5*).

The addition of a dc electric field to either crossflow or axial filtration introduces another mechanism, electrophoresis, which can move charged solutes away from the filter element. Beechold (*6*) was the first to describe an apparatus in which electrophoresis and electroosmosis were combined to purify colloidal solutions. He called the apparatus an "electroultrafilter." Several investigators subsequently reported combinations of crossflow filtration and electrofiltration (*7–10*). Mikhilin et al. (*11*) combined axial filtration and electrofiltration to separate polystyrene latex from an aqueous medium.

In the course of desalination research, Marcinkowsky and coworkers (*12*) added organic and inorganic polyelectrolytes to pressurized salt solutions which they found to form salt-filtering layer when the solutions were circulated past porous supports. To distinguish these from preformed films prepared by casting or other conventional procedures, these membranes were designated as "dynamically formed" or "dynamic" membranes. A wide assortment of additives was shown to form salt-filtering membranes including hydrous metal oxides, especially Zr(IV) oxide (ZrO_2), synthetic organic polyelectrolytes like poly-2-vinylpyridine (P-2VP), natural polyelectrolytes (e.g., humic acid and clay), and materials in water streams such as sewage and pulp mill wastes. The ZrO_2 membrane has been extensively studied while the others have received little attention. Subsequently, procedures to produce colloidal dispersions of uniform size and shape were reported by Matijevic (*13*), opening the possibility of forming dynamic membranes with reproducibilities better than those previously known.

OBJECTIVES

In this work a dc electric field and an axial filter were combined to separate bovine serum albumin (BSA) from a solution of disodium phosphate in distilled water at pH 8 using four different dynamic membranes. The objectives of the present study were: 1) to find four dynamic membranes which were stable upon application of a dc electric field; 2) to determine the effect of membrane formation variables on the mass and permeability of these dynamic membranes; 3) to determine the formation conditions giving the highest flux and rejection above 80% for BSA; and 4) to investigate the effects of BSA concentration, electric field strength, and rate of rotation on flux and BSA rejection. Since the zeta potential of BSA is negative at pH 8, the charge at the membrane must be negative to reduce the buildup of BSA.

EXPERIMENTAL APPARATUS AND METHODS

The Axial Electrofilter

The axial electrofilter (Fig. 1) consisted of a perforated stainless steel cylinder (18.5 cm long, 6.5 cm o.d. and 6.1 cm i.d.) which rotated within a stationary stainless steel cylinder of 8.1 cm i.d. Sixteen hundred holes of 0.1 cm diameter were drilled in the central 5 cm of the inner cylinder. This portion of the cylinder was covered by the membrane support, a 0.2-μm Versapor polymeric membrane (Gelman Instruments Inc., Ann Arbor, Michigan). The membrane was held in place along its length by a retaining clamp which fitted into a slot 0.2 cm deep and 5.5. cm long. This clamp was attached to the rotating cylinder by four screws, one in each corner. The ends of the membrane were held by a water-resistant tape (Scotch No. 850PTA). The membrane area was approximately 100 cm^2, but was determined for each new membrane from the measured length of membrane between the end tapes and the outside diameter of the perforated cylinder. The inner cylinder rotated in special seals which prevented electrical contact between the rotating and stationary cylinders. The inner cylinder was rotated by a variable speed motor fitted with a regulator to maintain a constant rpm. The maximum rotation rate in the present filter was 4000 rpm.

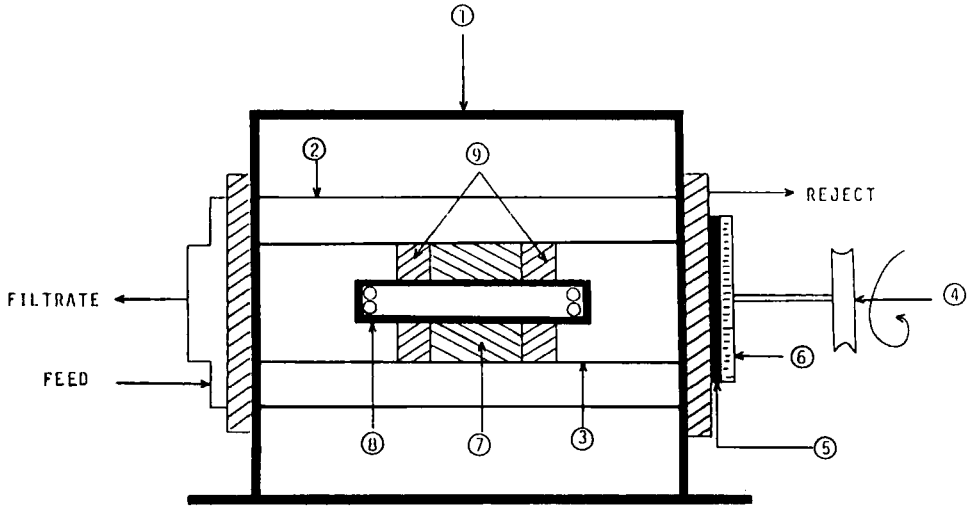

FIG. 1. The axial electrofilter. 1: Support frame. 2: Motionless housing. 3: Rotating cylinder. 4: Drive pulley. 5: Insulation. 6: Mercury chamber. 7: Versapor membrane. 8: Retaining clamp. 9: Tape.

A flow sheet of the apparatus is shown in Fig. 2. The feed, at constant temperature, was pumped to the annulus from a tank by a peristaltic pump with a pulsation damper. Reject was withdrawn constantly from the annulus at the end opposite the feed entry. Filtrate, drained by gravity from inside the inner cylinder, was recycled with the reject to maintain steady feed composition. The pressure at the point where the feed entered the annulus was maintained constant by adjusting the valve on the reject line. Gauge pressures of up to 210 kPa were used.

Finding Electrically-Stable Dynamic Membranes

A strip of Versapor was taped to the rotor, and the flux of a sodium chloride solution of 1.0×10^{-4} M concentration was measured at an rpm (N) of 2000 and a transmembrane pressure drop (ΔP) of 138 kPa. The dynamic membrane was then formed for 1 h, and the system was rinsed with distilled water. The sodium chloride solution was circulated again,

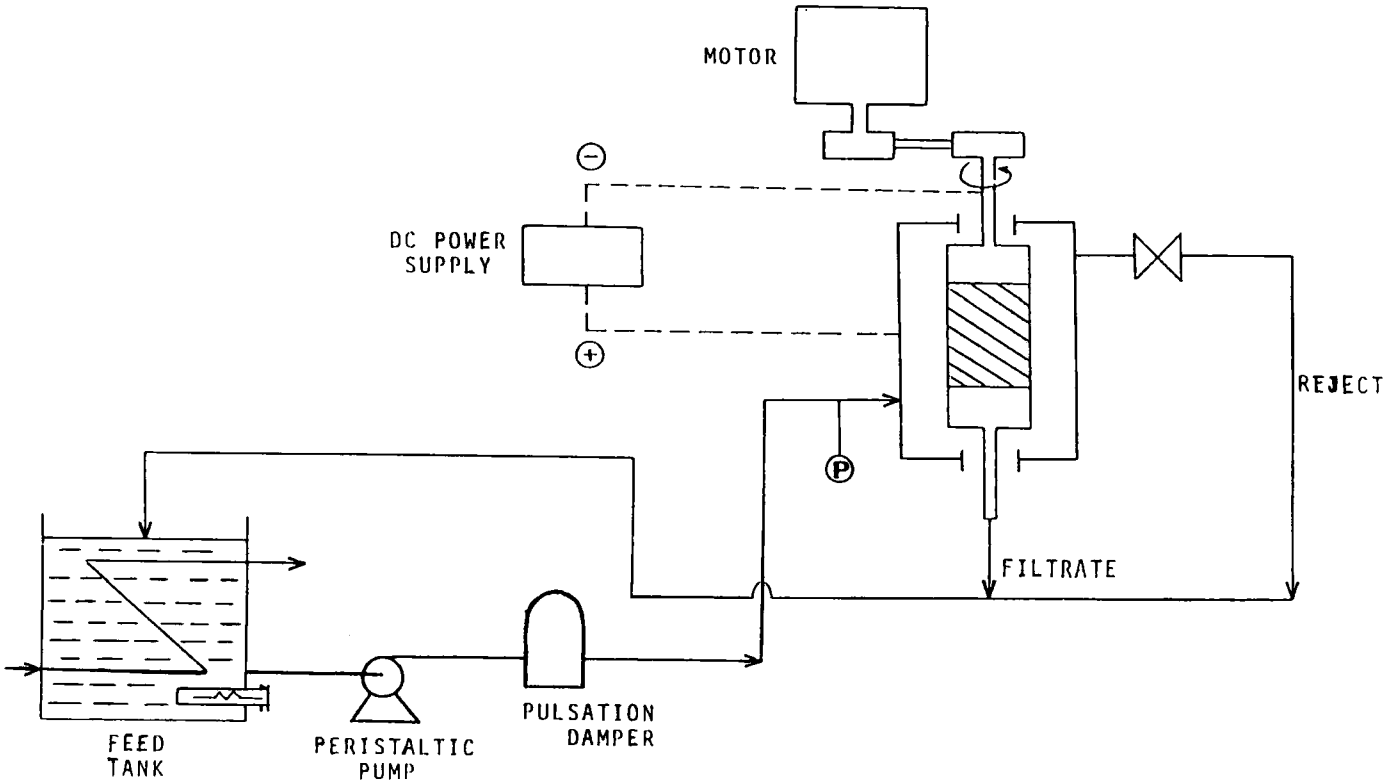

FIG. 2. Schematic diagram of flow loop.

and the flux was determined. Electric field strengths of 20, 40, and 60 V/cm were then applied sequentially without stopping the rotation, and the flux was determined after 30 min for each value. The rotor was the negative electrode while the stationary external cylinder was the positive electrode.

The following dynamic membranes were tested for electrical stability: ZrO_2, zinc oxide (ZnO), cadmium sulfide (CdS), calcium oleate (Ca-oleate), poly-2-vinylpyridine (P-2VP), sodium polystyrene sulfonate (SPSS), polyvinylpyrrolidone (PVP), and polyacrylic acid (PAA). The last two were unstable under a dc electric field. Calcium oleate and CdS were selected from the large number of materials investigated by Matijevic (*14, 15*). Of the stable additives, CdS, P-2VP, Ca-oleate, and ZrO_2 and gave the highest fluxes and were therefore used for the filtration of BSA.

Determination of the Mass of a Dynamic Membrane

The distilled water flux (J°) at N = 2000 rpm and ΔP = 138 kPa was measured with the Versapor in place without the dynamic membrane. The dynamic membrane was then formed for 1 h. The distilled water flux (J_0) at N = 2000 rpm and ΔP = 138 kPa was then determined after cleaning the dynamic membrane with distilled water for 5 min. Membranes were removed and immersed in 50 mL of 1.0 *M* nitric acid (Ca-oleate and CdS) or 50 mL of 1.0 *M* HCl (ZrO_2) for 24 h. Calcium and cadmium concentrations were measured with an atomic absorption spectrometer (Perkin-Elmer Model 403). The CdS and Ca-oleate weights were then calculated by stoichiometry. The weight of ZrO_2 was determined by the method of Green (*16*).

Determination of Optimum Dynamic Membrane Formation Conditions

The membrane-forming suspension of Zr(IV) oxide was prepared by adding zirconium oxychloride to 0.05 *M* NaCl in distilled water followed by adjustment of the pH with 1.0 *M* NaOH. The P-2VP suspension was formed by dissolving the material in aqueous HCl (pH 1.5) followed by pH adjustment by the addition of 1.0 *M* NaOH. The Ca-oleate and CdS suspensions were prepared by following the procedures outlined elsewhere (*14, 15*).

Factorial designs were used to determine the best formation conditions for ZrO_2, CdS, P-2VP, and Ca-oleate. The formation and rinsing at each set of formation conditons were followed by 3 h of filtration of BSA with measurement of the permeate flux and rejection at 30 min intervals. The operating conditions were C_0 = 0.05 wt%, pH 8, N = 2000 rpm, T = 30°C, and ΔP = 138 kPa, where C_0 is the feed concentraion and T is the temperature. The best formation conditions were considered to be those that yielded the highest flux accompanied by a rejection of at least 80% after 3 h of filtration.

BSA Adsorption and Concentration Measurement

The filtration mechanism of BSA was investigated by measuring the rate of adsorption of BSA on the dynamic membrane. The Versapor, with a rinsed dynamic membrane formed at its optimum conditions, was immersed in 20 mL unstirred BSA solution of known concentration. Samples of BSA were withdrawn and analyzed upon termination of the experiments. The BSA adsorbed was calculated from the BSA disappearance from solution. This procedure was repeated for a dynamic membrane which was exposed to 20 mL BSA solution. The BSA adsorbed on the dynamic membrane was obtained by difference.

Up to a concentration of 0.15 wt%, the BSA concentration was determined with a spectrophotometer (Bausch and Lomb Model DB) at a wavelength of 280 nm. Concentrations above 0.15 were determined with a total carbon analyzer (Beckman Model 915A).

THEORY OF MEMBRANE FORMATION

Dynamic membranes are formed as a result of solute accumulation at the surface of the primary membrane support during filtration. The mass of the accumulated solute is influenced by the properties of the suspension and the support and by the hydrodynamic conditions. By assuming the flow of filtrate through an incompressible cake to be laminar and that the resistance of the support is negligible, Ruth et al. (*17*) derived the

following relationship for filtration at constant pressure difference:

$$V/A = (2\Delta P_m t/\mu C_m \alpha)^{0.5} \quad (1)$$

where V = volume of filtrate collected in t seconds, mL
A = area of membrane, cm^2
μ = filtrate viscosity, g/cm · s
α = specific cake resistance, cm/g
C_m = solute concentration during formation of dynamic membrane, g/mL
ΔP_m = transmembrane pressure drop during dynamic membrane formation, dyn/cm^2

When solute rejection is 100%, the mass of accumulated solute per unit area, D_m, is

$$D_m = C_m V/A \quad (2)$$

or

$$D_m = (2\Delta P_m C_m t/\mu\alpha)^{0.5} \quad (3)$$

EXPERIMENTAL RESULTS AND DISCUSSION

Effect of Formation Parameters on Mass of Dynamic Membrane

Without rotation, the mass of dynamic membrane removed as a result of feed flow parallel to the medium was insignificant compared to the deposited mass. Since solute rejection was 100% for all dynamic membranes, a straight line on a plot of D_m versus $(\Delta P_m)^{0.5}$ is an indication of cake filtration. Figure 3 shows the mass of dynamic membrane per unit area after 1 h of formation versus $(\Delta P_m)^{0.5}$ at constant suspension concentration and no rotation for ZrO_2, Ca-oleate, and CdS dynamic membranes. The plot yields a straight line for all dynamic membranes in accordance with Eq. (3). This is also an indication that the dynamic membranes in Fig. 3 are incompressible between ΔP_m = 35 and 138 kPa.

Figure 4 shows the effect of the rate of rotation during membrane formation (N_m) on the mass of membrane deposited per unit area in 1 h for

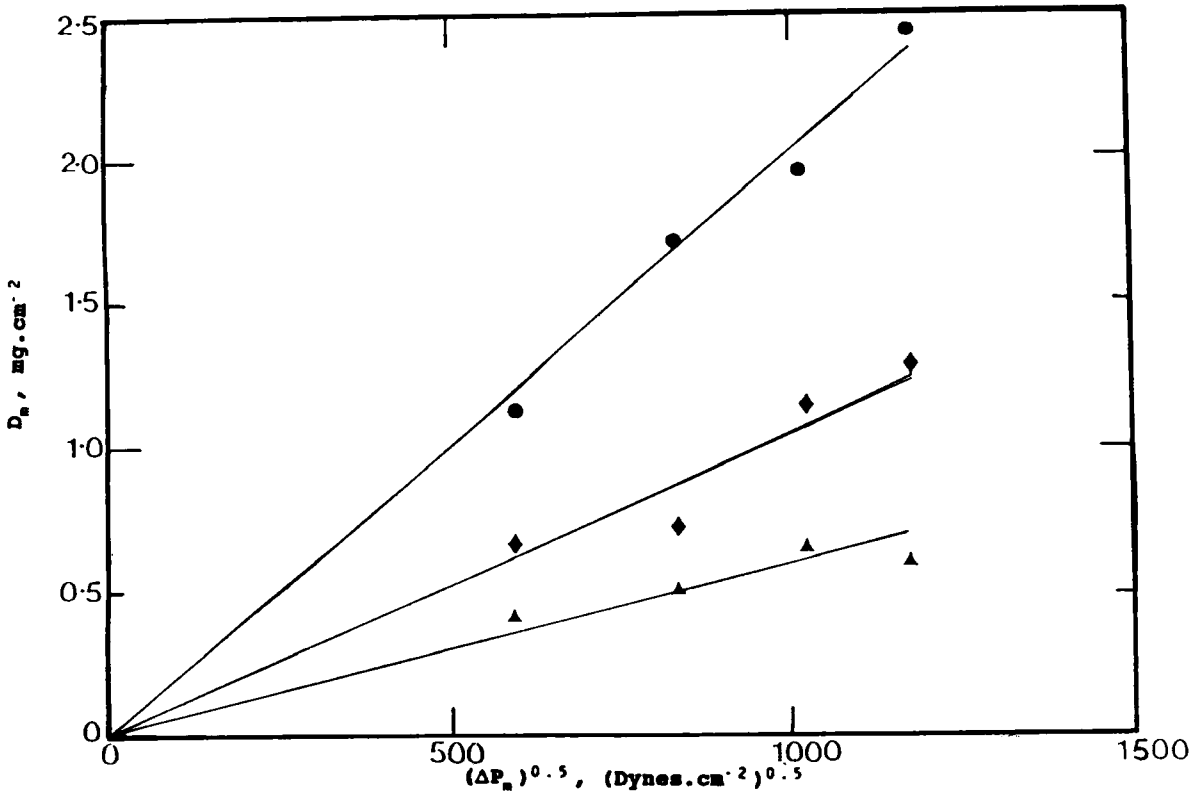

FIG. 3. Effect of pressure drop during membrane formation (ΔP_m) on mass per unit area of dynamic membrane (D_m) after 1 h of membrane formation.

	Dynamic membrane	C_m (g/mL)	pH_m
●	ZrO_2	2.0×10^{-3}	10.0
♦	CdS	2.9×10^{-4}	0.8
▲	Ca-oleate	3.0×10^{-5}	10.8

N_m = 0 rpm

ZrO_2 and CdS. For both dynamic membranes, D_m decreased with increasing N_m as increasing centrifugal force and shear stress reduced the accumulation of membrane-forming material on the support. Figure 4 also shows the effect of concentration of membrane-forming suspension (C_m) on D_m. For both membranes, D_m increased with increasing C_m in accord with Eq. (3).

Table 1 shows that increasing the pH of formation (pH_m) of the CdS suspension resulted in a decline in D_m while the opposite occurred for the ZrO_2 dynamic membrane. CdS particles were formed by decomposition of thioacetamide in nitric acid solutions containing cadmium nitrate. The extent of decomposition of thioacetamide decreases with increasing pH_m, leading to formation of smaller particles. Particles formed at pH_m 0.8 and 1.2 had an average size of 0.15 and 0.09 μm, respectively. The increase in CdS membrane resistance with increasing pH_m (Table 1) is attributable to decreasing CdS particle size with increasing pH_m since membrane pore size decreases with decreasing particle size. The average particle size of ZrO_2 particles increased from 0.05 to 0.1 μm when pH_m was increased from 3.5 to 10 at a concentration of 2.0×10^{-3} g/mL. The decrease of the ZrO_2 membrane resistance as the pH_m increased therefore corresponds to an increase in the average particle size as pH_m increased. A similar conclusion was reached by Freilich and Tanny (*18*).

Optimum Dynamic Membrane Formation Conditions

Table 2 contains summaries of the experimental results showing the effect of dynamic membrane formation conditions on the distilled water flux after membrane formation (J_0) and on the flux (J_{180}) and rejection of BSA (R_{180}) after 180 min of filtration for the CdS dynamic membrane.

Increasing the rate of rotation during membrane formation (N_m) resulted in an increase in both J_0 and J_{180} and a decline in R_{180}. This is indicative of a possible increase in pore size with increasing N_m.

For CdS, doubling the concentration resulted in an increase in J_0 as a result of an increase in CdS particle size (*15*) and in membrane pore size. For Ca-oleate, P-2VP, and ZrO_2 membranes, doubling C_m resulted in a decline in J_0 and J_{180} and an increase in R_{180} (*19*).

The formation of larger particle sizes with decreasing pH_m for CdS decreased membrane resistance (Table 1), causing J_0 to increase and R_{180} to decrease.

The size of CdS particles increased as the reaction time before membrane formation increased (*15*). This is reflected in J_m values for different

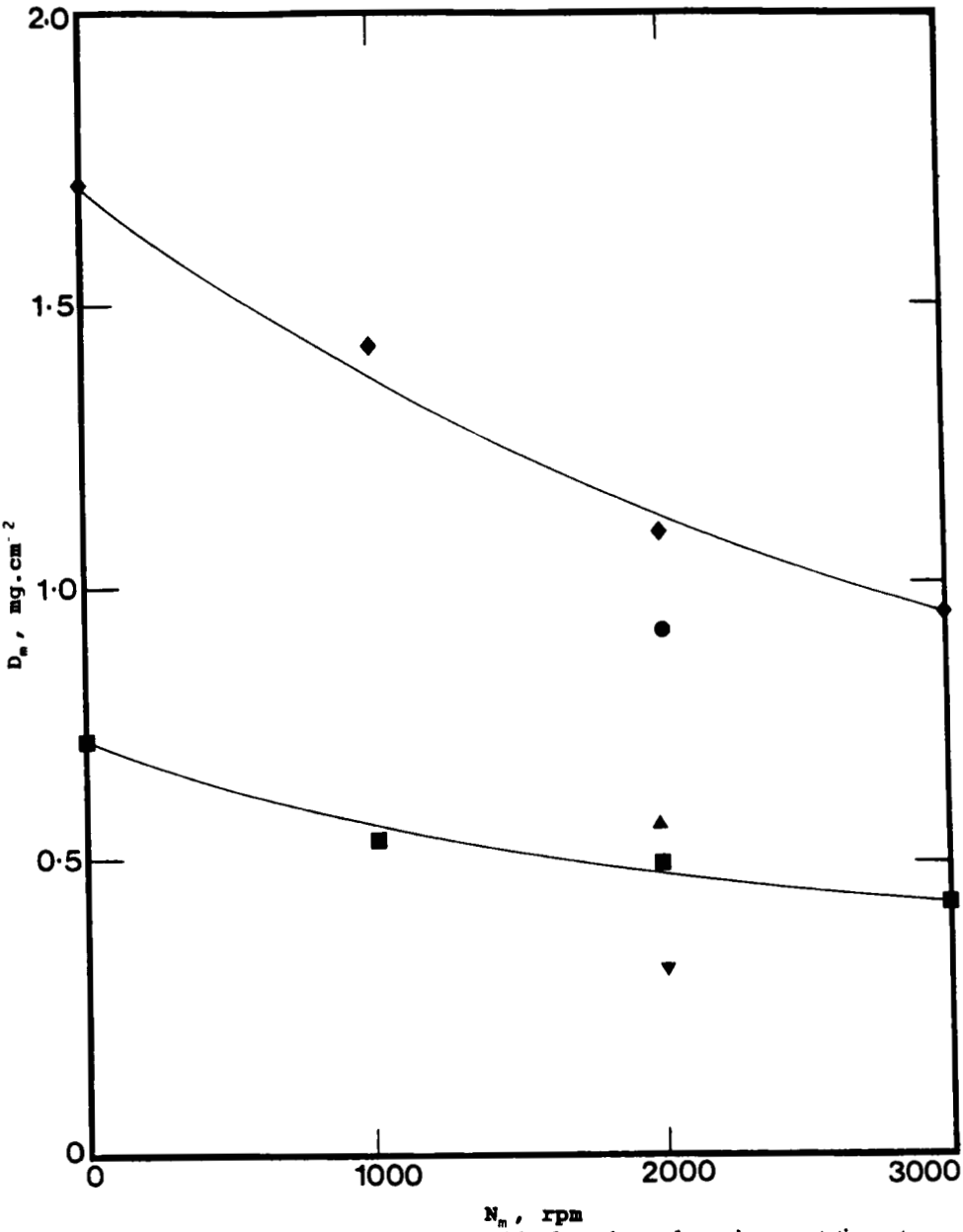

FIG. 4. Mass of membrane per unit area after 1 h of membrane formation vs rotation rate during membrane formation.

	Dynamic membrane	C_m (g/mL)	pH_m
♦	ZrO_2	2.0×10^{-3}	10.0
●	ZrO_2	1.0×10^{-3}	10.0
▲	ZrO_2	5.0×10^{-4}	10.0
■	CdS	2.9×10^{-4}	0.8
▼	CdS	1.45×10^{-4}	0.8
		ΔP_m = 69 kPa	

TABLE 1
Effect of Suspension pH on Dynamic Membrane Properties
(ΔP_m = 69 kPa, N_m = 0 rpm, T = 30°C)

Dynamic membrane	pH_m	C_m (g/mL)	D_m (mg/cm^2)	$\alpha \times 10^{-14}$ (cm/g)
CdS	0.8	1.45×10^{-4}	0.42	4.08
	1.2	1.45×10^{-4}	0.29	8.57
ZrO_2	3.5	2.0×10^{-3}	0.92	11.70
	10.0	2.0×10^{-3}	1.70	3.44

TABLE 2
Effects of CdS Dynamic Membrane Formation Conditions on Flux and Rejection of BSA at ΔP_m = 69 kPa

N_m (rpm)	pH_m	t_m (h)	C_m (g/mL)	J_0 (cm/s)	J_{180} (cm/s)	R_{180} (%)
2000	0.8	1	2.90×10^{-4}	0.044	0.0180	54
2000	0.8	1	1.45×10^{-4}	0.036	0.0172	77
0	0.8	1	1.45×10^{-4}	0.028	0.0157	82
0	1.2	1	1.45×10^{-4}	0.025	0.0153	87
0	1.2	6	1.45×10^{-4}	0.035	0.0179	61
0	1.2	24	1.45×10^{-4}	0.041	0.0190	38

t_m, shown in Table 2. A more porous membrane was formed as the size of CdS particles increased with t_m, leading to an increase in J_m and J_{180} and a decline in R_{180}.

The optimum formation conditions for each dynamic membrane are summarized in Table 3.

Comparison of Dynamic Membrane Performance

Figure 5 shows the filtrate flux and rejection versus time for BSA at N = 2000 rpm, ΔP = 138 kPa, C_0 = 0.05 wt%, pH 8, and T = 30°C. The best membrane was CdS, while ZrO_2, which has been widely used, gave the

TABLE 3
Optimum Dynamic Membrane Formation Conditions for BSA
(formation time, 1; T, 30°C)

Dynamic membrane	pH_m	C_m (g/mL)	N_m (rpm)	ΔP_m (kPa)	J_0 (cm/s)
CdS	0.8	1.45×10^{-4}	0	69	0.028
Ca-oleate	10.8	3.00×10^{-5}	2000	69	0.045
P-2VP	2.0	1.00×10^{-4}	2000	69	0.047
ZrO_2	3.5	2.00×10^{-3}	0	69	0.010

lowest flux. For all membranes the flux declined with time to a nearly constant value after 120 min of filtration. The rejection was low at the beginning of experimentation and then increased to over 80% and remained essentially constant after 120 min.

Figure 6 shows the time variation of the amount of BSA absorbed on CdS for bulk concentrations of 0.05 and 0.05 wt%. The rate of adsorption was rapid at first and then fell until after about 120 min the rate was nearly zero. The adsorption data suggest that the increase in BSA rejection was due to pore closure as a result of adsorption. The rejection increased until equilibrium was reached. Rejection and flux profiles similar to those in Fig. 5 were observed by Fane et al. (*20*) during filtration of BSA. They also attributed the increase in rejection with time to reduction in pore size due to adsorption.

The amount of membrane-forming additive in the feed and filtrate after 180 min of filtration was determined to be less than 5% of the mass of membrane deposited on the support for each of Ca-oleate, CdS, and ZrO_2. This means that BSA did not react with any of the additives to effect their removal.

Effect of BSA Concentration on the Flux and Rejection

Figure 7 illustrates the effect of increasing BSA concentration on flux and rejection for the CdS membrane. The flux decreased with increasing concentration, but above C_0 = 5.0 wt% the flux was nearly invariant with concentration. The BSA rejection also decreased with increasing feed concentration to a nearly constant value above C_0 = 0.5 wt%. Similar results were obtained for the ZrO_2 membrane. Above C_0 = 5.0 wt%, the flux

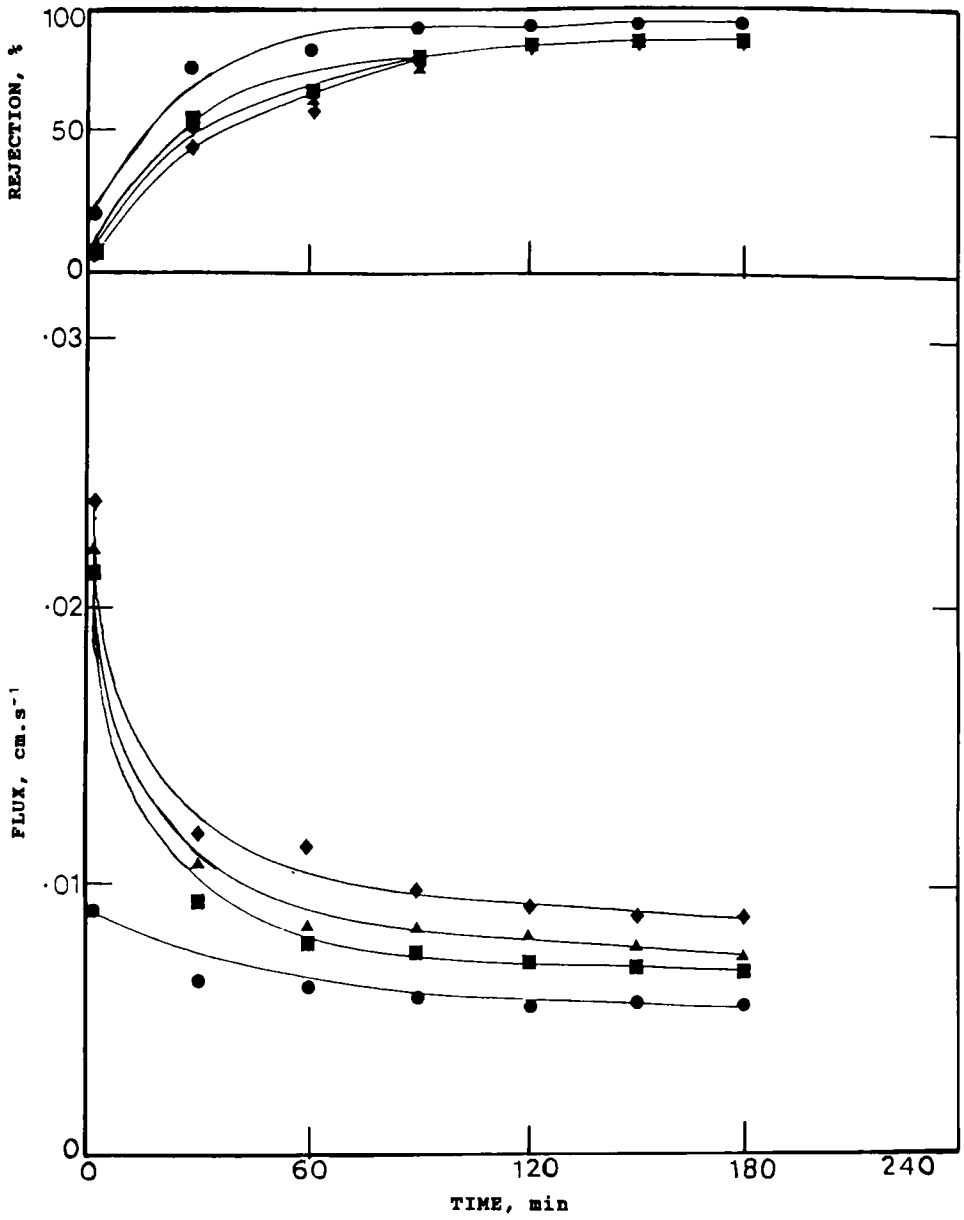

FIG. 5. Variation of flux and rejection with time with different dynamic membranes. BSA conditions: C_0 = 0.05 wt%, N = 2000 rpm, pH 8, T = 30°C, ΔP = 138 kPa.

	Dynamic membrane
◆	CdS
▲	Ca-oleate
■	P-2VP
●	ZrO_2

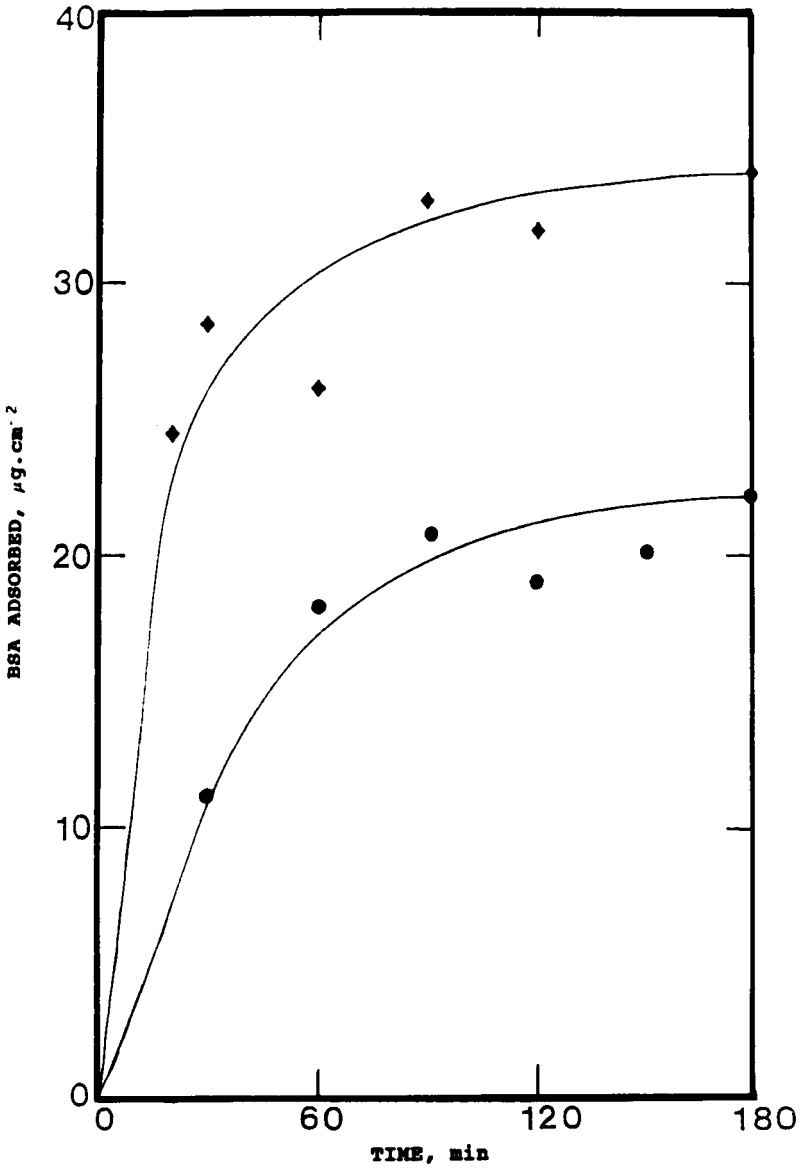

FIG. 6. Adsorption rate of BSA with CdS dynamic membrane.

	C_0 (wt%)
●	0.05
♦	0.50

T = 30°C

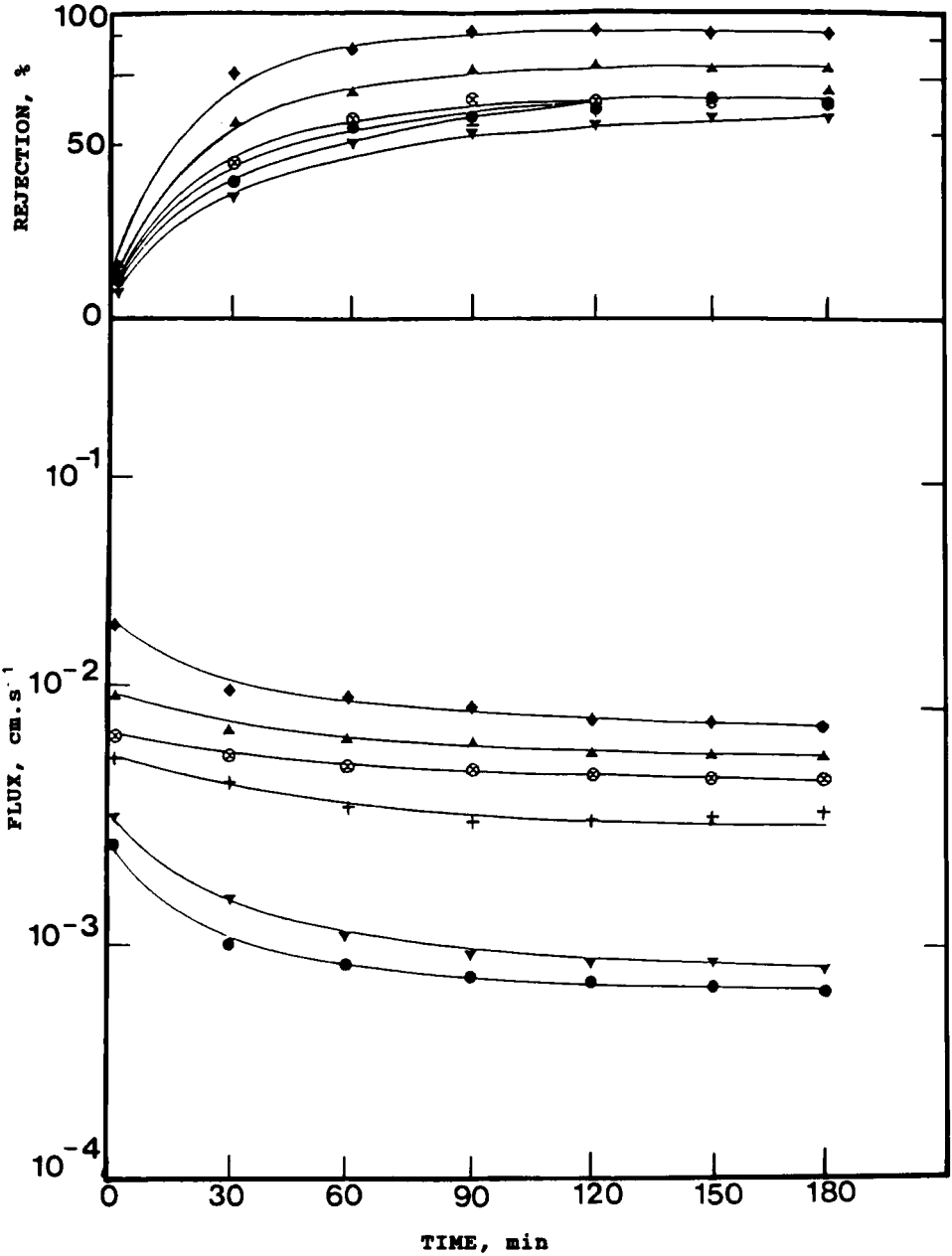

FIG. 7. Variation of flux and rejection with time. Effect of concentration with CdS dynamic membrane. BSA conditions: N = 2000 rpm, pH 8, T = 30°C, ΔP = 138 kPa.

	C_0 (wt%)
♦	0.05
▲	0.2
⊗	0.5
+	1.0
▼	5.0
●	10.0

was nearly the same for both membranes. The flux and rejection levels at the beginning and after 120 min. were similar to those obtained by Fane et al. (*20*) for BSA at C_0 = 0.05 and 0.1 wt% and a lower pH of 7.4 using an Amicon XM-100 membrane. Adsorption of BSA on the XM-100 membrane was also demonstrated by them.

For membranes that are partially permeable to a specific macromolecule, Anderson and Brannon (*21*) outlined a mechanism to explain declining rejection with increasing bulk concentration when the flux is small enough such that diffusion is predominant over convection. In such a case, interactions between the macromolecules and pore walls during filtration were said to lead to the distances between the macromolecules being considerably greater inside the pores than in the bulk solution. In the absence of adsorption, an increase in the bulk concentration, therefore, leads to increased penetration of macromolecules through the pores and a decline in rejection. Anderson and Brannon (*21*) derived a theoretical relationship between rejection and bulk concentration which showed the rejection to decline by 20% when the concentration was increased to 10 wt% from infinite dilution in the absence of adsorption and concentration polarization. The presence of adsorption and concentration polarization may cause the effect of bulk concentration on the rejection to be completely different from that predicted by Anderson and Brannon. Solute adsorption within the pores, for example, causes the effective pore size to decrease. If adsorption increases with increasing concentration, the rejection may increase or decrease as the bulk concentration is increased, depending on whether pore size reduction by adsorption or increased solute penetration as a result of macromolecule–pore wall interaction is predominant. The occurrence of concentration polarization may cause the rejection to decline more severely than expected from an increase in bulk concentration alone.

The effects of time and concentration on rejection and flux observed in Fig. 7 may be explained using a hypothesis based on 1) classification of the pores into three groups of small, medium, and large pores due to nonuniformity of the pores; 2) adsorption within all the pores; and 3) concentration polarization at the surfaces of the small and medium groups of pores. The pore classification hypothesis is analogous to a model proposed by Fane et al. (*22*) who observed pore sizes in an Amicon XM-100 membrane ranging from 105 to 250 Å and then proceeded to derive a flux relationship based on two groups of small and large pores.

The Stokes-Einstein diameter of a BSA molecule is 74 Å (*23*). Assume an adsorption process at low bulk concentrations in which rigid spherical BSA molecules are adsorbed on the wall of a cylindrical pore. This im-

plies that all pores with diameter, d, $\leq$ 148 Å (small pores) become blocked almost immediately, while resistance to the permeation of BSA molecules within pores with 148 $< d <$ 222 Å (medium pores) increases with time. BSA molecules, however, freely permeate pores with $d >$ 222 Å (large pores). For the Amicon XM-100 membrane, Fane et al. (*22*) determined through scanning electron microscopy that pores less than 222 Å constituted 95% of all pores. As stated above, the filtration performance of this membrane resembled that of the dynamic membranes employed in this work. It is, therefore, assumed that adsorption and concentration polarization at the small and medium pores were the dominant mechanisms affecting the performance of the CdS membrane. The increase in rejection as a result of adsorption was, therefore, counteracted by a decline in rejection due to concentration polarization. Steady-state rejection, the magnitude of which was dependent on the relative effects of adsorption and concentration polarization, was reached when both mechanisms equilibrated. Because concentration polarization was minimal at low bulk concentrations, the predominance of adsorption caused high steady-state rejection.

As the bulk concentration increased, the adsorption rate and concentration polarization at the small and medium pores both increased. However, the negative effect of concentration polarization on the rejection was larger than the positive effect of adsorption. The result was a decline in rejection as the bulk concentration increased. The rejection became constant around C_0 = 0.5 wt% when the effects of adsorption and concentration polarization were balanced.

Even while maintaining a constant bulk concentration, Fane et al. (*20*) observed a similar influence of concentration polarization on rejection as adsorption increased during filtration of BSA at different solution pH. The rejection decreased from pH 3 to a minimum around pH 5 and then increased to a maximum at pH 9 with Amicon XM-100 as the membrane. Since the isoelectric pH of BSA is 4.7, repulsion between BSA molecules decreased, and hence adsorption increased as pH increased from 3 to 5 and also as the pH decreased from 9 to 5. Therefore, like the results in Fig. 7, rejection declined as the adsorption rate increased, with the minimum value realized when the adsorption rate was maximum.

Adsorption in the large pores (without significant concentration polarization) is the controlling mechanism when the large pores predominate. In this case the rejection increases with increasing concentration as Reihanian et al. (*24*) observed for BSA filtration with an Amicon XM-300 membrane. For the XM-300 membrane, Fane et al. (*22*) showed that the large pores, i.e., pores larger than 222 Å, constitute about 65% of all pores

and that 90% of the flow went through these pores. In this case, concentration polarization in the small and medium pores was largely irrelevant to the determination of the overall rejection.

These considerations may be generalized as follows for filtration of a macromolecule with diameter a. For membranes with pore diameters predominantly between a and $3a$, there is an amount of adsorption beyond which the rejection decreases. For a membrane in which pores with $d > 3a$ predominate, increased adsorption increases the rejection.

Since adsorption shrinks the pores and concentration polarization increases the hydraulic resistance opposing flow, the filtrate flux decreases. When the bulk concentration is increased, these mechanisms become more pronounced and the flux declines. For concentrations above some limit (here 5 wt%), hydraulic resistance of the BSA layer becomes predominant and the flux becomes independent of the membrane permeability.

Effect of Rotation Rate on Flux and Rejection

Figure 8 shows the effect of rotation rate on the flux and rejection for BSA at C_0 = 0.05 wt%, pH 8, and ΔP = 138 kPa. The flux increased with increasing rotation rate and then declined beyond N = 2000 rpm. Measurements demonstrated that the inner cylinder was filled with liquid to about 80% of its volume. This accumulated liquid rotated as a solid body, causing the transmembrane pressure difference to decline with increasing rotation. Turkson (*25*) showed that the decrease in the transmembrane pressure difference was proportional to the square of the rotation rate. In Fig. 8 the increase in flux suggests that the decline in hydraulic resistance with rotation rate was predominant over the decline in pressure difference up to N = 2000 rpm. The reverse was true beyond N = 2000 rpm, and the flux decreased. Without liquid holdup inside the rotating cylinder, Lopez-Leiva (*4*) and Vigo and Uliana (*5*) observed an increase in flux with rotation rate until the flux became constant beyond N = 2000 rpm during ultrafiltration of BSA and emulsions, respectively.

Figure 8 also shows an increase in BSA rejection with rotation rate and then a decline beyond N = 2000 rpm. If the surface concentration decreases with increasing rotation rate, the permeate concentration will decrease and the rejection will increase. Nakao et al. (*26*) found that this occurred by measuring directly the surface concentration of ovalbumin with increasing velocity over the membrane. At C_0 = 0.5 wt%, increasing the

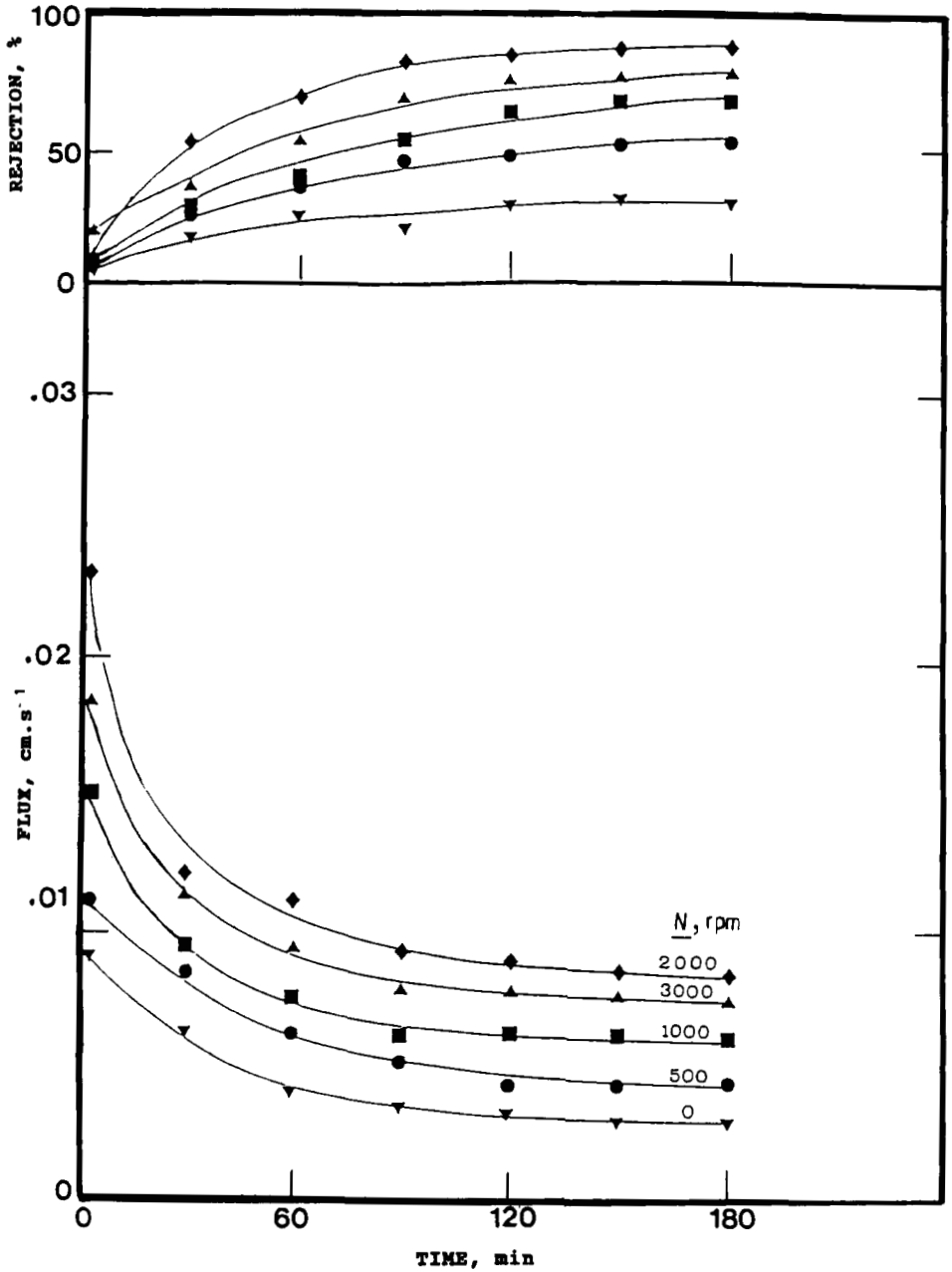

FIG. 8. Variation of flux and rejection with time. Effect of rotation rate with CdS dynamic membrane. BSA conditions: C_0 = 0.05 wt%, pH 8, T = 30°C, ΔP = 138 kPa.

feed velocity from 35 to 55 cm/s decreased the surface concentration from about 4 to 2.5 wt%. The drop in rejection beyond $N = 2000$ rpm might have been caused by deformation of the molecules which allowed them to pass through the pores more easily, a hypothesis partly supported by the work of Bell and Dunnill (*27*), who found the molecular size of soya protein decreased with increasing shear rate.

Effect of Electric Field Strength on Flux and Rejection

Figures 9 to 11 illustrate the effect of dc electric field strength on filtrate flux and rejection for BSA at $C_0 = 0.05$ wt% and pH 8 for CdS, Ca-oleate, and ZrO_2 dynamic membranes. Similar results were obtained for the P-2VP membrane. The electric field strength levels were 0, 10, 20, and 30 V/cm. The flux increased with field strength at all times while the rejection was nearly constant. The increase in flux was greatest for CdS and least for Ca-oleate.

Yukawa et al. (*8*) attributed an invariant rejection–field strength relationship at higher feed velocity to the gel layer being so thin as to be practically unaffected by field strength. If this assumption were true, the filtrate flux would not vary with field strength. The fact that the flux was a strong function of the field strength even as the rejection remained constant suggests a significant reduction in polarization. The application of an electric field could have removed adsorbed molecules from the pores as well as reducing polarization. The former reduces rejection while the latter increases it. Hence, rejection may increase or decrease with field strength depending upon the controlling mechanism. At $C_0 = 0.05$ wt%, the effects balance and the rejection remains constant with field strength as the flux increases. At $C_0 = 0.1$ wt%, however, the flux and rejection both increased with increasing field strength, thus suggesting that reduction of polarization controls at higher concentrations (*19*).

A plot of the flux at steady state versus the electric field strength should, according to Bier (*7*), be linear with a slope approximately equal to the electrophoretic mobility of the solute. Figure 12 shows that the relationship between J_{180} and E is approximately linear for all membranes. The slopes from Fig. 12, which are listed in Table 4 as S_A, show order of magnitude agreement with the mobility. For BSA at pH 8, the mobility measured with a microzone electrophoresis cell (Beckman-Spinco Model R-101) was 1.6×10^{-4} cm^2/V · s. The electroosmotic contribution to the flux could not be accounted for, and this might explain why the slope for CdS is greater than mobility. As Radovich et al. (*10*) point out, the assumption

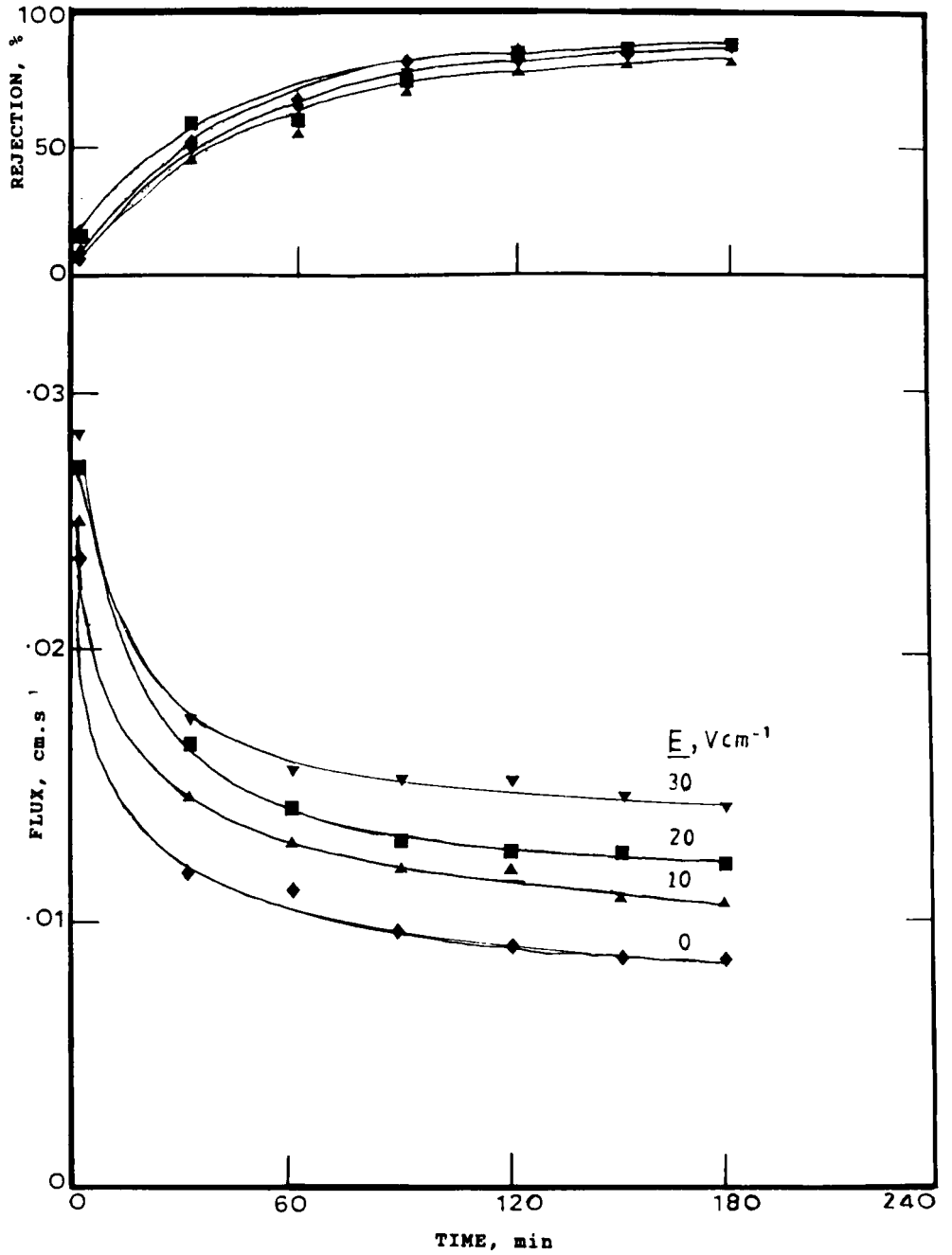

FIG. 9. Variation of flux and rejection with time. Effect of electric field strength with CdS dynamic membrane. BSA conditions: C_0 = 0.05 wt%, N = 2000 rpm, pH 8, T = 30°C, ΔP = 138 kPa.

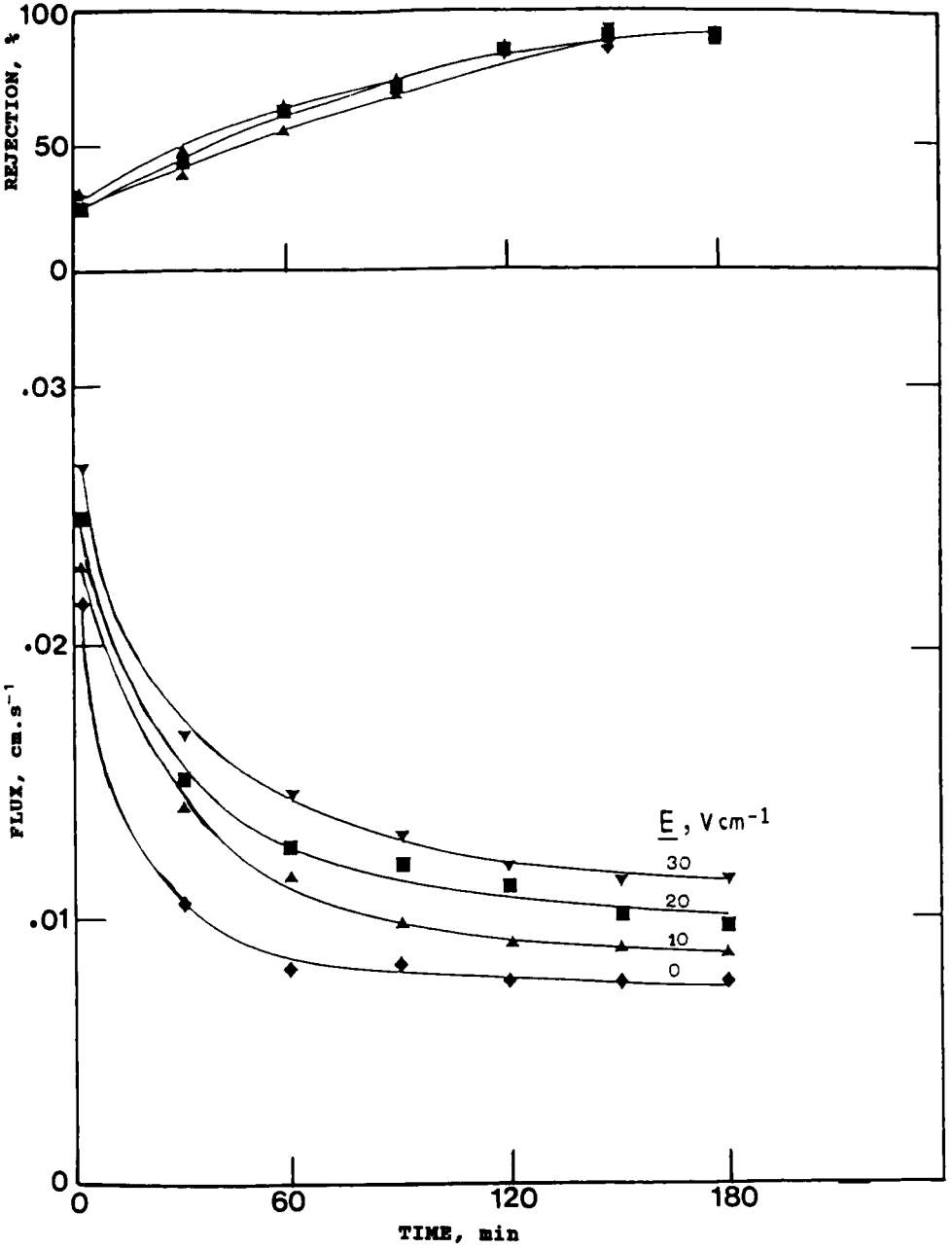

FIG. 10. Variation of flux and rejection with time. Effect of electric field strength with Ca-oleate dynamic membrane. BSA conditions: C_0 = 0.05 wt%, N = 2000 rpm, pH 8, T = 30°C, ΔP = 138 kPa.

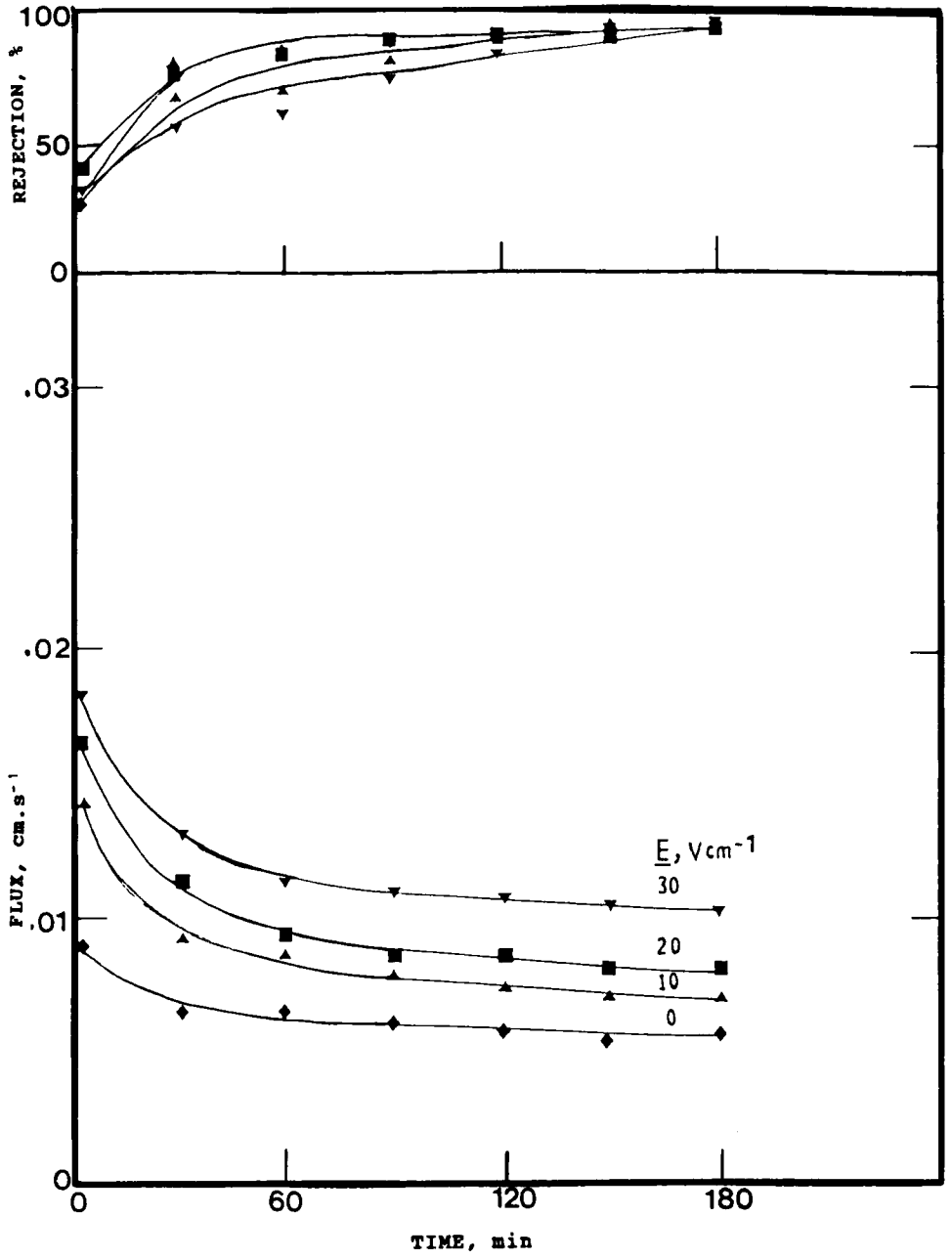

FIG. 11. Variation of flux and rejection with time. Effect of electric field strength with ZrO_2 dynamic membrane. BSA conditions: C_0 = 0.05 wt%, N = 2000 rpm, pH 8, T = 30°C, ΔP = 138 kPa.

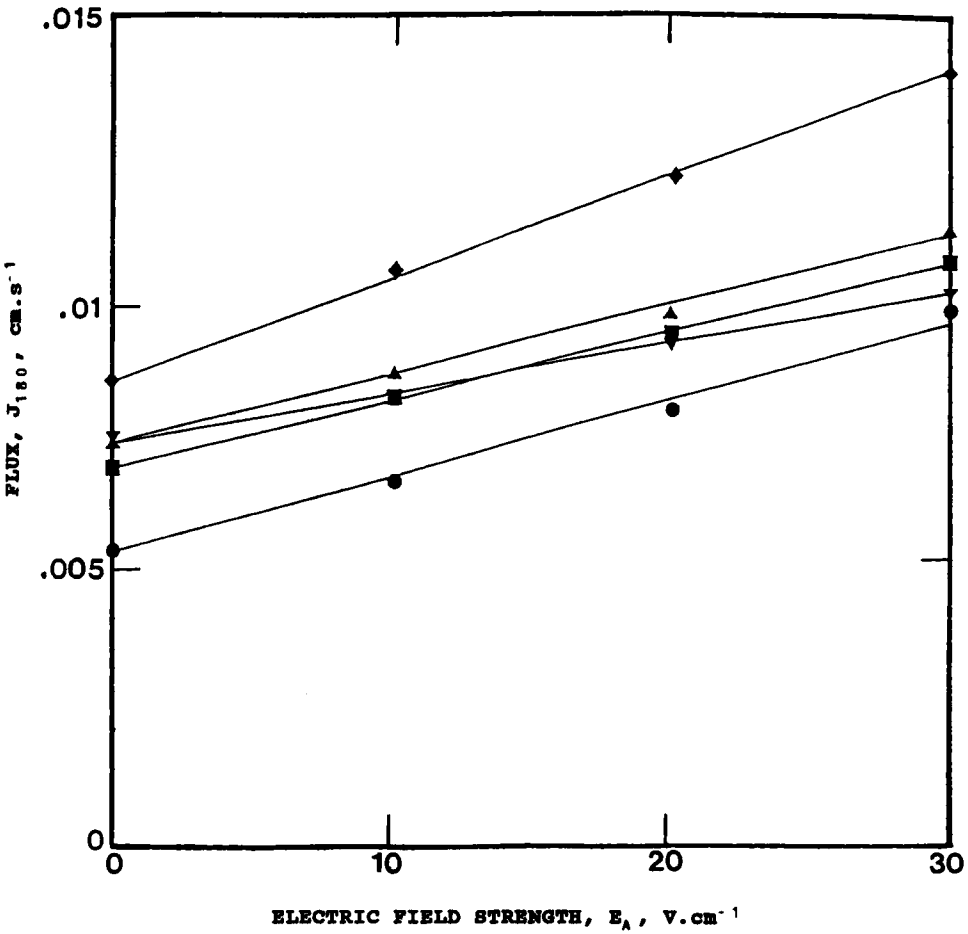

FIG. 12. Flux after 180 min vs electric field strength for BSA with different dynamic membranes. BSA conditions: N = 2000 rpm, pH 8, T = 30°C, ΔP = 138 kPa.

	Dynamic membrane	C_0 (wt%)
♦	CdS	0.05
▲	Ca-oleate	0.05
●	ZrO_2	0.05
■	P-2VP	0.05
▼	CdS	0.10

that S_A is equal to the electrophoretic mobility implies that the effect of E on the solute concentration at the membrane surface is negligible. This is incorrect and might also be one of the reasons for the differences between S_A and the electrophoretic mobility.

The average electric resistance across the annular gap during filtration, R_A, was determined by measuring simultaneously the voltage difference and the current. The resistance R_A includes the resistances of the support, the dynamic membrane, the BSA layer, and the fluid in the annular gap. Comparison of the values of R_A and S_A, tabulated in Table 4, shows that S_A is inversely related to R_A, hence the lower the electrical resistance of the dynamic membrane, the smaller the voltage drop across it and the larger the field in the annular gap. It is the field in the annular gap which moves the BSA molecules away from the membrane.

Table 4 also shows S_A to be dependent upon the BSA feed concentration. With CdS, S_A declined from 1.9×10^{-4} to 0.9×10^{-4} cm^2/V · s when the feed concentration increased from 0.05 to 0.1 wt%. Similar observations were reported by Yukawa et al. (*8*) and Wakeman and Tarleton (*9*) during electrofiltration of gelatin and antase, respectively. The R_A values in Table 4 show that the voltage drop across the BSA layer increased with increasing feed concentration. In view of these results, the data obtained by Radovich et al. (*10*), which showed that the slopes from plots of J versus E increased not only with increasing concentration but also with declining feed flow rate, are surprising. Indeed, Radovich and Sparks (*28*) acknowledged "a large voltage drop" across a deposited paint film resulted in a decrease in "field strength in the retentate compartment." One would expect, therefore, that the voltage drop would increase with an increase in solute deposition, resulting in a decline in the slopes of plots of J versus E as the concentration increased and the feed flow rate declined, the opposite of the results obtained by Radovich et al. (*10*).

TABLE 4
Electrical Resistances and Slopes from Plots of J_{180} versus E (S_A) and J_{180} versus E_E (S_E) (N = 2000 rpm, ΔP = 138 kPa, pH 8, T = 30°C)

Dynamic membrane	C_0 (wt%)	R_A (Ω)	S_A (cm^2/V · s)	S_E (cm^2/V · s)
CdS	0.05	39.2	1.90×10^{-4}	2.48×10^{-4}
Ca-oleate	0.05	53.7	1.27×10^{-4}	2.20×10^{-4}
P-2VP	0.05	56.2	1.30×10^{-4}	2.09×10^{-4}
ZrO_2	0.05	44.8	1.43×10^{-4}	2.37×10^{-4}
CdS	0.10	69.8	0.90×10^{-4}	2.00×10^{-4}

The conductivity of the BSA solution was measured as 6.3×10^{-5} mho/cm (*19*), and resistance of the BSA solution in the annular gap was computed to be 30 Ω. Assuming that the BSA solution is in series with the combined electrical resistance of the support, the dynamic membrane and the BSA layer permit the calculation of the effective electric field in the annular gap at the outer surface of the inner cylinder, E_E:

$$E_E = \Delta V_E / r_i \ln (r_o/r_i) \tag{4}$$

where r_o is the inside radius of the outer cylinder, r_i is the outer radius of the inner cylinder, and ΔV_E, the effective voltage difference, is given by:

$$\Delta V_E = (R_{BSA}/R_A)\Delta V \tag{5}$$

where ΔV is the applied voltage drop.

The slope of a plot of J_{180} versus E_E should be approximately the same for all operating condtions. Figure 13 shows plots of J_{180} versus E_E with the slopes given in Table 4 as S_E. The agreement between S_E values for different dynamic membranes and operating conditions is good. The mean and 95% confidence interval of the S_E values in Table 4 is $2.23 \times 10^{-4} \pm 0.25 \times 10^{-4}$ cm^2/V · s. For the experimentally determined electrophoretic mobility, the confidence interval is $1.60 \times 10^{-4} \pm 0.14 \times 10^{-4}$ cm^2/V · s. The difference is most probably due to electroosmosis in the dynamic membrane since electroosmosis has been determined to be negligible in the BSA layer (*10*).

CONCLUSIONS

(1) Calcium oleate and cadmium sulfide, additives which have never been used for the formation of dynamic membranes, were employed, together with zirconium oxide and poly-2-vinylpyridine dynamic membranes for the filtration of bovine serum albumin (BSA) solutions. The membranes were formed by a cake filtration mechanism. Formation conditions were found which gave the highest flux accompanied by a rejection above 80% during filtration of BSA at pH 8, N = 2000 rpm, ΔP = 138 kPa, and T = 30°C. The best dynamic membrane was CdS while ZrO_2, which has been used extensively, was the worst.

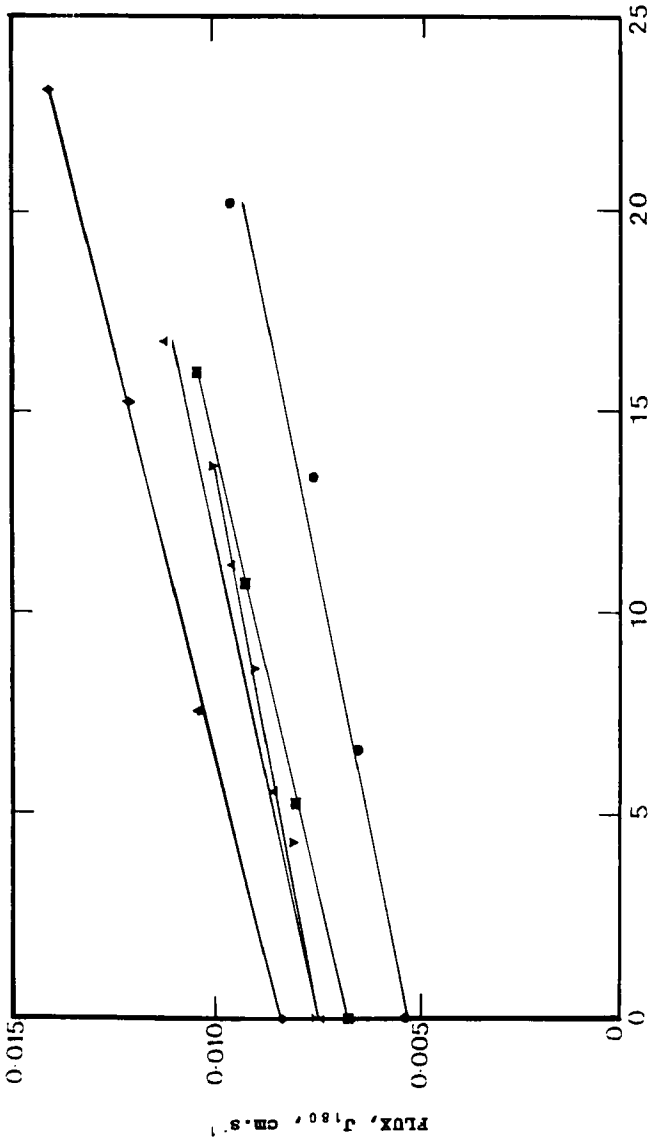

FIG. 13. Flux after 180 min vs effective field strength for BSA with different dynamic membranes. BSA conditions: N = 2000 rpm, pH 8, T = 30°C, ΔP = 138 kPa.

	Dynamic membrane	C_0 (wt%)
◆	CdS	0.05
▲	Ca-oleate	0.05
●	ZrO_2	0.05
■	P-2VP	0.05
▼	CdS	0.10

(2) During filtration of BSA the flux fell while the rejection increased until both attained almost constant values after 120 min. Experimental data revealed an increase in adsorption with time which resulted in a decline in the hydraulic permeability of the dynamic membrane. The effective pore size of the membrane therefore decreased with time, causing the BSA rejection to increase.

(3) Investigation of the effects of bulk concentration, rotation rate, and electric field strength on the flux and rejection showed that flux increased with N and E and declined with C_0. The flux declined beyond N = 2000 rpm and was independent of the dynamic membrane above C_0 = 5.0 wt%. The rejection increased with N up to 2000 rpm and then fell with a further increase of N. At high N and low concentration, the rejection was invariant with E, while at lower N and higher C_0, the rejection increased with increasing E. The rejection declined with increasing C_0 and then became constant above C_0 = 0.5 wt%.

(4) Values of the flux after 180 min. (J_{180}) of filtration increased linearly with the electric field strength, with the rate of increase being dependent on the electrical resistance of the dynamic membrane and BSA layer. Good agreement was obtained between the rate of increase of flux with electric field strength for all dynamic membranes and operating conditions when J_{180} was plotted against the effective electric field strength instead of the applied electric field strength.

SYMBOLS

a	macromolecular diameter (cm)
A	area of the filter medium (cm^2)
C_m	concentration of dynamic membrane-forming additive (g/mL)
C_0	bulk solute concentration (wt%)
d	pore diameter (cm)
D_m	mass of dynamic membrane per unit area (g/cm^2)
E	electrical field strength (V/cm)
E_E	effective electrical field strength (V/cm)
J_0	distilled water flux through dynamic membrane at N = 2000 rpm and ΔP = 138 kPa (cm/s)
J°	distilled water flux through Versapor polymeric membrane at N = 2000 rpm and ΔP = 138 kPa (cm/s)
J_{180}	flux after 180 min of filtration (cm/s)
N	rate of rotation (rpm)
N_m	rate of rotation during formation of dynamic membrane (rpm)

R_A	electrical resistance of Versapor support, dynamic membrane, solute layer, and feed in the annular gap (ohm)
R_{BSA}	electrical resistance of BSA solution (ohm)
r_i, r_o	inside radius of outer cylinder, outside radius of rotating cylinder (cm)
R_{180}	rejection of BSA after 180 min of filtration
S_A	slope of plot of J_{180} versus E ($cm^2/V \cdot s$)
S_E	slope of plot of J_{180} versus E_E ($cm^2/V \cdot s$)
t	time (s)
T	temperature (°C)
t_m	reaction time before beginning of CdS dynamic membrane formation (s)
V	volume of filtrate (mL)
α	specific cake resistance (cm/g)
ΔP	transmembrane pressure difference (kPa)
ΔP_m	transmembrane pressure difference during formation of dynamic membrane (dyn/cm^2)
ΔV	voltage difference (V)
ΔV_E	effective voltage difference (V)

Acknowledgments

This work was supported by the Natural Sciences and Engineering Research Council of Canda. A. K. Turkson was supported by a fellowship from the Government of Ghana.

REFERENCES

1. A. I. Zhevnovatyi, *Int. Chem. Eng.*, (4), 124–128 (1964).
2. A. K. Bhagat and C. R. Wilke, *Lawrence Radiation Laboratory Report UCRL-16574*, 1966.
3. T. K. Sherwood, P. L. T. Brian, and R. E. Fisher, *Ind. Eng. Chem., Fundam.*, *6*, 2–12 (1967).
4. M. Lopez-Leiva, *Desalination, 35*, 115–128 (1980).
5. F. Vigo and C. Uliana, *Sep. Sci. Technol., 21*, 367–381 (1986).
6. H. Beechold, in *Colloid Chemistry, 1* (J. Alexander, ed.), Chemical Catalog Company, 1926.
7. M. Bier, in *Electrophoresis* (M. Bier, ed.) Academic, New York, 1959, Chap. 15.
8. H. Yukawa, K. Shimura, A. Suda, and A. Maniwa, *J. Chem. Eng. Jpn., 16*, 305–311 (1983).
9. R. J. Wakeman and E. S. Tarleton, *Filtr. Sep., 23*, 174–176 (1986).

10. J. M. Radovich, B. Behnam, and C. Mullon, *Sep. Sci. Technol., 20,* 315-329 (1985).
11. J. A. Mikhlin, M. E. Weber, and A. K. Turkson, *J. Sep. Processes Technol., 3,* 16-24 (1982).
12. A. E. Marcinkowsky, K. A. Kraus, A. O. Phillips, J. S. Johnson, and A. J. Shor, *J. Am. Chem. Soc., 88,* 5744-5746 (1966).
13. E. Matijevic, *Pure Appl. Chem., 50,* 1193-1210 (1978).
14. R. Nemeth and E. Matijevic, *Kolloid-Z. Z. Polym., 245,* 497-507 (1971).
15. E. Matijevic and D. M. Wilhelmy, *J. Colloid Interface Sci., 86,* 476-484 (1982).
16. D. E. Green, *Anal. Chem., 29,* 370-372 (1948).
17. B. F. Ruth, G. H. Montillon, and R. E. Montonna, *Ind. Eng. Chem., 25,* 76-82 (1933).
18. D. Freilich and G. B. Tanny, *J. Colloid Interface Sci., 77,* 369-378 (1980).
19. A. K. Turkson, "Electro-Ultrafiltration with Rotating Dynamic Membranes," PhD Thesis, McGill University, Montreal, 1985.
20. A. G. Fane, C. J. D. Fell, and A. G. Waters, *J. Membr. Sci., 16,* 211-224 (1983).
21. J. L. Anderson and J. H. Brannon, *J. Polym. Sci., Polym. Phys. Ed., 19,* 405-421 (1981).
22. A. G. Fane, C. J. D. Fell and A. G. Waters, *J. Membr. Sci., 9,* 245-262 (1981).
23. L. Tinghul, K. Chan, T. Matsuura, and S. Sourirajan, *Ind. Eng. Chem., Prod. Res. Dev., 23,* 116-124 (1984).
24. H. Reihanian, C. R. Robertson, and A. S. Michaels, *J. Membr. Sci., 16,* 237-258 (1983).
25. A. K. Turkson, "Tengential Flow Electrofiltration," MEng Thesis, McGill University, Montreal, Quebec, 1980.
26. S.-I. Nakao, T. Nomura, and S. Kimura, *AIChE J., 25,* 615-622 (1979).
27. D. J. Bell and P. Dunnill, *Biotechnol . Bioeng., 24,* 1271-1285 (1982).
28. J. M. Radovich and R. E. Sparks, in *Ultrafiltration Membranes and Applications* (A. R. Cooper, ed.), Plenum, New York, 1980, pp. 249-268.

Received by editor July 21, 1988